

Studies on the process of throughfall drop generation in forest canopies

樹冠における林内雨滴の形成メカニズムに関する研究

南光 一樹

Studies on the process of throughfall drop generation in forest canopies

Kazuki Nanko

The University of Tokyo

2007

Contents

1. Introduction	8
1.1 Backgrounds	8
1.1.1 Surface erosion process at forest floor	8
1.1.2 Canopy interception process	9
1.2 Research history of throughfall drop study	10
1.2.1 Open rainfall drops	10
1.2.2 Measuring techniques of drops	10
1.2.3 Previous studies of throughfall drops	11
1.2.4 Problems of previous studies of throughfall drops	11
1.3 Objectives of this study	12
2. Methods for measuring and calculating throughfall drops	14
2.1 Measuring method of throughfall drops	14
2.1.1 Requirements for instruments to measure throughfall drops	14
2.1.2 Measuring principle of the LD gauge	15
2.1.3 Development of the LD gauge	16
2.1.4 Improvement of the LD gauge	18
2.2 Calculating method of throughfall drops	20
3. Characteristics of throughfall drops: A field observation of throughfall in an unmanaged Japanese cypress plantation	22
3.1 Introduction	22
3.2 Materials and methods	23
3.3 Results and discussions	25
3.4 Conclusions	30
4. Influence of canopy species and meteorological factors for throughfall drop generation: A field observation of throughfall under three canopy species	32
4.1 Introduction	32
4.2 Materials and methods	33

4.3	Results	36
4.4	Discussion	42
4.5	Conclusions	47
5.	Influence of canopy structures for throughfall drop generation: An indoor experiment with a transplanted Japanese cypress tree	48
5.1	Introduction	48
5.2	Materials and Methods	49
5.2.1	An indoor experiment	49
5.2.2	Method of analysis	52
5.2.3	Analysis procedure	54
5.3	Analysis I: Effect of the distance from the trunk for throughfall drop generation	57
5.3.1	Results	57
5.3.2	Discussion	66
5.4	Analysis II: Effect of the branch pruning for throughfall drop generation	68
5.4.1	Results	68
5.4.2	Discussion	77
5.5	Conclusion	79
6.	Summary and Conclusion	81
7.	Acknowledgements	84
8.	References	86

List of Figures

1.1.	An unmanaged Japanese cypress plantation with little surface cover, no undergrowth and little litter.	9
1.2.	Structures of this paper.	13
2.1.	An example of the temporal variations of output voltage from the laser sheet receiver. Each decrease of the output voltage was caused by the two drops with different drop size and velocity.	16
2.2.	Front and top views of the LD gauge version 1. And top view of the sampling hole. Units are millimeters.	17
2.3.	Calibration relationship between the interception rate and the glass sphere diameter (<i>vertical line</i>) for six different sizes and the water drop diameter (<i>circle</i>) for four different sizes. ...	19
2.4.	Comparison of the 1-h rainfall intensity between the tipping-bucket (<i>bar graph</i>) and the LD gauge (<i>line graph</i>) data. Each figure shows the raindrop capture rate and correlation coefficient.	19
2.5.	Top and front views of the LD gauge version 2. Units are millimeters.	21
3.1.	Study site locations.	23
3.2.	Temporal transition in rainfall intensity and drop size. The <i>broken lines</i> indicate 3.31 mm, the maximum diameter of open rainfall drops in this observation. <i>P</i> indicates the total precipitation for rainfall events, Event 1 (a) and Event 2 (b).	26
3.3.	Comparison of the 1-h rainfall intensity between R1 and R2 measured with the tipping-bucket raingauges.	27
3.4.	Drop size distributions of open rainfall and throughfall in Event 2, based on drop volume (a) and based on kinetic energy (b).	28
3.5.	Drop size distributions of throughfall in Event 1 and Event 2, based on drop volume (a) and based on kinetic energy (b).	29
3.6.	a Relationship of the cumulative precipitation and cumulative kinetic energy during Event 1 and Event 2. At the <i>circle</i> and <i>square</i> , the slope changes gently, and at the <i>triangle</i> the slope changes abruptly. b Temporal variation in throughfall rainfall intensity in Event 1. Each <i>symbols</i> links to the <i>symbols</i> in the top figure.	31

4.1.	Study site locations.	33
4.2.	Distribution of all hourly-based data sets on rainfall intensity and 5-min minimum wind speed. The <i>dashed lines</i> indicate boundaries of rainfall intensity and wind speed. The data in the <i>upper right</i> were not considered in this study.	35
4.3.	Temporal variations in wind speed, rainfall intensity, and drop size at four observation sites in Event A. The drop size is shown in the contour plans with 0.3 mm in diameter class and 0.5 mm in minimum diameter per 10 min. The <i>dashed lines</i> indicate 3.5 mm, which was the maximum diameter class of open rainfall drops in Event A; <i>P</i> indicates the total precipitation for Event A.	37
4.4.	Temporal variations in wind speed, rainfall intensity, and drop size at four observation sites in Event B. The <i>dashed lines</i> indicate 4.4 mm, which was the maximum diameter class of open rainfall drops in Event B.	38
4.5.	Temporal variations in wind speed, rainfall intensity, and drop size at four observation sites in Event C. The vertical scales of wind speed and rainfall intensity are twice larger than Fig. 4.3 and 4.4. The <i>dashed lines</i> indicate 4.7 mm, which was the maximum diameter class of open rainfall drops in Event C.	39
4.6.	a Drop size distributions (DSDs) at the four observation sites during the overall observation period, with 0.3 mm in diameter class and 0.5 mm in minimum diameter. Each DSD was normalized by the respective water volume. b Cumulative DSD. The <i>dashed horizontal line</i> indicates the 50% line of cumulative DSD.	40
4.7.	a Drop size distributions (DSDs) at the four observation sites for three meteorological conditions, categorized in Fig. 4.2. b Cumulative DSD. The <i>dotted horizontal lines</i> indicate the 50% lines of cumulative DSD. The <i>dashed vertical lines</i> indicate the D_{50} of CD under the condition <i>Low</i> , 2.87 mm in diameter.	41
4.8.	DSD difference at the three throughfall observation sites for the three meteorological conditions. The DSD difference was calculated by subtracting the open-DSD from the throughfall-DSD of Fig. 4.7a. Positive values indicate that throughfall was higher than open rainfall.	43
4.9.	Leaf apices of CY, CD, and SO. SO had a large surface area per leaf. CY and CD had fine scale-like leaves.	45
4.10.	Schematic diagram illustrating the components generating throughfall-DSD.	46
5.1.	Transplanted trees in the rainfall simulator.	50
5.2.	Four canopy structures.	51
5.3.	32 measuring points under the canopy.	51
5.4.	DSDs of the applied rainfall of Rain-L and Rain-H.	53
5.5.	Dominating area of each measuring point.	55
5.6.	An example of dataset of the applied rainfall and throughfall; the temporal variation of rainfall intensity, drop size, and kinetic energy. Throughfall data were measured at [150] on line-4 of T1.	56
5.7.	Temporal variations of rainfall intensity of throughfall of T1 and the applied rainfall. The <i>upper</i> shows the mean throughfall intensity. The <i>lower</i> shows the mean value at 8 measuring	

points with each distance from the trunk.	58
5.8. Throughfall amount in relation to the distance from the trunk of T1 in Rain-L.	58
5.9. Throughfall intensity in relation to the distance from the trunk of T1, during stable phases in Rain-L and Rain-H. <i>Dotted lines</i> represent the rainfall intensity of the applied rainfall.	59
5.10. Throughfall-DSD at 32 all measuring points during the stable phase in Rain-H. The canopy stage was T1.	61
5.11. DSDs of the applied rainfall and throughfall during the stable phase in Rain-H. Each throughfall-DSD was at [40], [150], [200] on line-4. The canopy stage was T1.	60
5.12. DSDs of the applied rainfall and throughfall at each distance from the trunk of T1 during the stable phases in Rain-L and Rain-H. Each throughfall-DSD was drawn using all drops measured at eight measuring points.	62
5.13. Throughfall D_{50} in relation to the distance from the trunk of T1 during the stable phases. <i>Broken lines</i> indicate the applied rainfall D_{50} in Rain-L (the <i>lower</i>) and the in Rain-H (the <i>upper</i>).	62
5.14. Volume ratio of drops with each diameter class in relation to the distance from the trunk, during the stable phases in Rain-L (the <i>left</i>) and Rain-H (the <i>right</i>).	63
5.15. Relationship between drop diameter and drop velocity of total drops of T1 measured at 32 measuring points during the stable phase in Rain-H. The <i>Solid line</i> indicates the terminal velocity of drops and the <i>broken line</i> indicates assumed drop velocity when drops fell from a height of 2 m. Each assumed drop velocity was set out by Zhou et al. (2002).	64
5.16. The distribution of throughfall drop velocity with diameters > 3 mm of T1. The number of drops was totally counted at 32 all measuring points during the stable phase in Rain-H. <i>Gray belts</i> represent terminal velocity and assumed drop velocity when drops fall from 2 m high, both were set out by Zhou et al. (2002).	64
5.17. Throughfall kinetic energy in relation to the distance from the trunk of T1 during stable phases in Rain-L and Rain-H. <i>Broken lines</i> represent the kinetic energy of the applied rainfall.	65
5.18. Throughfall unit kinetic energy in relation to the distance from the trunk of T1 during stable phases.	67
5.19. Temporal variations of rainfall intensity of throughfall for each canopy structure. Starting from the <i>top</i> , the figure shows throughfall intensity at [40], [100], [150], and [200], respectively.	69
5.20. Throughfall amount in relation to the canopy structures with the distance from the trunk in Rain-L. The <i>Broken line</i> represents the rainfall amount of the applied rainfall.	70
5.21. Throughfall intensity in relation to the canopy structures with the distance from the trunk during stable phases in Rain-L and Rain-H. The <i>Broken lines</i> represent the applied rainfall intensity.	70
5.22. Throughfall-DSD of each canopy structure during stable phases in Rain-L and Rain-H. Starting from the <i>top</i> , the figure shows throughfall intensity at [40], [100], [150], and [200], respectively.	72
5.23. Throughfall D_{50} in relation to the canopy structures with the distance from the trunk during stable phases in Rain-L and Rain-H. The <i>Broken lines</i> represent D_{50} of the applied rainfall.	

.....	71
5.24. Volume ratio of drops with each diameter class in relation to the canopy structures during the stable phases in Rain-L and Rain-H. Starting from the <i>top</i> , the figure shows throughfall intensity at [40], [100], [150], and [200], respectively.	73
5.25. The distribution of throughfall drop velocity with diameters > 3 mm with each canopy structure. The number of drops was totally counted at 32 all measuring points during the stable phase in Rain-H. <i>Horizontal belts</i> represent the expected drop velocity when drops fell from 2–5 m high, respectively, and terminal velocity, set out by Zhou et al. (2002).	74
5.26. The distribution of throughfall drop velocity with diameters > 3 mm with the distance from the trunk. The figures were separately drawn using Fig. 5.25.	75
5.27. Throughfall kinetic energy in relation to the canopy structures with the distance from the trunk, during stable phases in Rain-L and Rain-H. <i>Broken lines</i> represent the kinetic energy of the applied rainfall.	76
5.28. Throughfall unit kinetic energy in relation to the canopy structures with the distance from the trunk during stable phases in Rain-L and Rain-H. <i>Broken lines</i> represent the unit kinetic energy of the applied rainfall.	78

List of Tables

2.1.	Specifications of the laser sensor.	15
2.2.	Specifications of the LD gauge version 1.	17
2.3.	Specifications of the LD gauge version 2.	21
3.1.	Study sites and instrument set-up.	25
3.2.	Rainfall events.	25
3.3.	Comparison of open rainfall and throughfall in Event 2.	28
3.4.	Comparison of two throughfall events in Event 1 and 2.	29
4.1.	Characteristics of throughfall sites.	34
4.2.	Rainfall events.	34
4.3.	D_{50} and drop number of each sites under three meteorological conditions.	40
4.4.	The abundance ratio of drops exceeding 2 mm in diameter in Fig. 4.8.	44
5.1.	Characteristics of the applied rainfall.	53
5.2.	Dominating ratio of each measuring point with the distance from the trunk.	55
5.3.	CU of throughfall intensity of T1 during the stable phases in Rain-L and Rain-H.	59
5.4.	The number and the ratio of total drops with velocities < 6.5 m s ⁻¹ at each distance from the trunk.	65
5.5.	The number and the ratio of total drops with velocities > 7.5 m s ⁻¹ with each canopy structure at each distance from the trunk.	76

Chapter 1

Introduction

1.1 Backgrounds

1.1.1 Surface erosion process at forest floor

Control of soil erosion is an important resource management objective for the sustainability of long-term productivity and protection of aquatic ecosystems. Soil erosion is a two-phase process consisting of the detachment of individual soil particles from the soil mass and their transport by erosive agents such as running water (Morgan, 2005). Surface erosion can be triggered by the impact of a raindrop on the soil surface. Splash detachment caused by raindrop impact is an important first step in the sequence leading to soil loss and subsequent sediment transport (e.g., Ellison, 1944; Meyer, 1981; Sharma and Gupta, 1989; van Dijk et al., 2002b; Kinnel, 2005). The drop impacts directly cause splash detachment as a detaching agent (e.g., Bubenzer and Jones, 1971; Cruse and Larson, 1977; Gabet and Dunne, 2003; Erpul et al., 2005) and indirectly cause overland flow through decreasing an infiltration rate of soil as a transport agent (e.g., Agassi et al., 1985; Keren, 1989; Betzalel et al., 1995; Salles et al., 2000; Foloy and Silburn, 2002; Singer and Shainberg, 2004). Rainfall kinetic energy has often been suggested as an indicator of rainfall erosivity (Mihara, 1951; Free, 1960). Soil particle detachment caused by raindrop impact has been incorporated in some soil erosion process models such as the Morgan-Morgan-Finney (Morgan et al., 1984, revised in Morgan, 2001) and EUROSEM (Morgan et al., 1998) models. Splash detachment rate is positively correlated with rainfall kinetic energy (Free, 1960; Morgan, 1978; Quansah, 1981). Therefore the estimation of rainfall erosivity is required to study the soil erosion process.

Surface erosion generally does not occur in forests because forest litter and undergrowth form a protective surface cover from the drop impacts. However, soil erosion is a serious problem for some plantations, including eucalyptus (*Eucalyptus exserta*) plantations in southern China (Zhou et al., 2002) and northern Portugal (Terry, 1996), coffee plantations in the tropics (Hanson et al., 2004),



Figure 1.1 An unmanaged Japanese cypress plantation with little surface cover, no undergrowth and little litter.

teak (*Tectona grandis*) plantation in Thailand (Bell, 1987), and unmanaged Japanese cypress (*Chamaecyparis obtusa*) plantations (e.g., Akenaga and Shibamoto, 1933; Kawana et al., 1963; Miura et al., 2002; Miura et al., 2003).

Unmanaged Japanese cypress plantations have little surface cover (Fig. 1.1), in part because cypress litter decomposes into small pieces within two or three months (Sakai and Inoue, 1988). Furthermore, weak sunlight penetration through canopies results in poor development of forest undergrowth (Magarisawa et al., 1992). Soil splash detachment is a predominant factor contributing to surface erosion in Japanese cypress plantations (Miura et al., 2002). To clarify surface erosion in such forests with no surface cover, it is necessary to determine the drop size distribution and the kinetic energy of throughfall, because the canopy produces large drops and promotes the erosive potential of the drops by increasing their kinetic energy (Chapman, 1948).

1.1.2 Canopy interception process

The interception of precipitation by vegetation canopies is a major component of the surface water balance in watersheds. The rainfall applied to forest canopies partly passes through the canopies and the rest was caught and stored in canopies. The stored rainwater redistributed to three components; throughfall, stemflow, and the interception loss. Many interception studies have been conducted

worldwide, in tropical areas (e.g., Asdak et al., 1998), in temperate broad-leaved forests (e.g., Hörmann et al., 1996), and in temperate coniferous forests (e.g., Klaassen et al., 1998), by both observational and modeling methods (summarized in Link et al., 2004). Among interception process models (Rutter et al., 1971; Gash, 1979), a two-layer stochastic model (Calder, 1996; Calder et al., 1996; Hall et al., 1996) accounts for the gradual wetting of a vegetation canopy by raindrops and water then dripping from an upper canopy layer onto a lower one. The interception losses were dependent not only upon the intensity of rainfall events (Crockford and Richardson, 2000; Murakami, 2006) but also upon the size of the drops (Calder, 1996), and differences in interception losses among canopy species were explained by the size of throughfall drops (Hall, 2003). Evaluating the drop size distribution (DSD) of throughfall is necessary for input into stochastic models in order to better understand the interception process.

1.2 Research history of throughfall drop study

1.2.1 Open rainfall drops

Many researchers have studied the drop size distribution of open rainfall. Some studies have calculated the drop kinetic energy (e.g., Hudson, 1965; Wischmeier and Smith, 1978; Kinnel, 1982; Epema and Riezebos, 1984; Banzai et al., 1999; Salles et al., 2002) and, more recently, discussed the accuracy of radar raingauges (e.g., Atlas et al., 1984; Yoshino, 1994; Brandes et al., 1999). Marshall and Palmer (1948) developed a widely used drop size distribution model that depends on rainfall intensity. It is known that the drop size distribution varies among rainfall types (Sempere-Torres et al., 1994; Uijlenhoet and Stricker, 1999).

Drops of open rainfall have terminal velocities. Drop terminal velocity is strongly influenced by drop size (Laws, 1941). Many researchers have empirically related the terminal velocity of falling raindrops to drop diameters (e.g., Laws, 1941; Gunn and Kinzer, 1949; Best, 1950; Mihara, 1951; van Dijk et al., 2002) and determined physical equations (e.g., Beard and Pruppacher, 1971; Beard, 1976).

1.2.2 Measuring techniques of drops

There are two types of methods for monitoring drop sizes and distributions as noted in Eigel and Moore (1983) and Martin and Joss (2000); a manual method and an automatic method. There are mainly four manual methods; the stain method introduced by Wisner (1895) and reviewed by Hall (1970); the flour method reported by Bentley (1904) and described by Laws and Parson (1943); the glass plate method reported by Mihara (1951); and the immersion method reported by Fuchs and Petranoff (1937). The manual methods have simple and easy measuring principles. However, the manual methods lack continuity of observation data and require much time to calculate drop size distribution (Hall and Calder, 1993; Yamada et al., 1996).

On the other hand, there are mainly three automatic methods; the photographic method uses a

particle spectrometer (Barthazy et al., 1998); the momentum method uses a Joss-Waldvogel disdrometer (Joss and Waldvogel, 1967) and a force transducer (Jayawardena and Rezaur, 2000); and the optical method uses an optical disdrometer (Illingworth and Stevens, 1987; Yamada et al. 1996; Salles et al. 1999; Martin and Joss 2000). The momentum method is commonly used to measure drop size distributions and drop kinetic energies in open rainfall. Drop kinetic energy is directly measured and drop diameter is calculated from kinetic energy using the relationship between drop diameter and drop terminal velocity. The optical method directly measures respective drop size and velocity.

1.2.3 Previous studies of throughfall drops

There have been relatively few studies, in contrast to open rainfall, that have examined throughfall drops. The drop size distribution and drop kinetic energy of throughfall were studied in field observations and indoor experiments (e.g. Chapman, 1948; Tsukamoto, 1966; Mosley, 1982; Vis, 1986; Brandt, 1989; Brandt, 1990). Chapman (1948) was the first study to show the result that the canopy produced large raindrops and promoted raindrops' erosive potential by increasing their kinetic energy. These studies derived that throughfall had larger drops than open rainfall and had clearly different characteristics for drop size distribution. Furthermore, they showed that throughfall drop size distribution was independent of canopy species (Vis, 1986; Brandt, 1989) and rainfall intensity (Chapman, 1948; Mosley, 1982; Vis, 1986); thus throughfall had a typical drop size distribution (Tsukamoto, 1966; Brandt, 1989).

Based on the assumption, Brandt (1990) consulted a model calculating throughfall kinetic energy. A two-level stochastic model has been used on the assumption that throughfall drop size distribution was constant within each rainfall event (Hall, 2003).

1.2.4 Problems of previous studies of throughfall drops

Although previous studies established a theory for throughfall drop size distribution, they had some problems. First, previous studies measured throughfall drops using the manual methods. The measuring data lacked continuity; and thus there were insufficient measurements of the changes in throughfall drop size distribution during temporal variations in meteorological factors. Furthermore, the calculation of drop kinetic energy was conceptual because of fragmentary drop data and calculation of leafdrip drops velocity using empirical or theoretical calculations from previous studies (e.g. Laws, 1941; Gunn and Kinzer, 1949; van Dijk et al., 2002a). Hall and Calder (1993) used the optical disdrometer, which was a kind of automatic optical method, and showed that throughfall drop size distribution varied among canopy species in tropical regions. Therefore, continuous drop measuring may make new findings for throughfall drop size distribution.

Second, rainfall intensity was only estimated as the variation factors of throughfall drop size distribution. For open rainfall, the drop size distribution strongly depends on rainfall intensity but also depends on wind speed. Erpul et al. (1998) observed open rainfall drop size became larger in windy condition with an experiment involving simulated rain in a wind tunnel. The other meteorological factors would affect throughfall drop size distribution.

Third, there was no optimized instrument to measure throughfall drops. The automatic techniques by the optical method are required for continuous measurements of throughfall drops. Hall and Calder (1993), which was the only study measuring throughfall drops with the optical method, alternately measured drops in the open field and under canopies with an optical disdrometer. More than two instruments are required to compare drop data between in and out of forests, or among canopy species. Previous instruments using the optical method did not meet multiple simultaneous measurements because they were large size and expensive.

Accordingly, the studies lack to estimate the influence of canopy species, canopy structures, meteorological factors, and spatial variability for drop size distribution and drop kinetic energy of throughfall. Detailed studies were needed to clarify the characteristics of throughfall drop generation.

1.3 Objectives of this study

Objective of this study are to develop the optimized system measuring throughfall drops and to clarify the process for throughfall drop generation in forest canopies. The author supposed meteorological factors and canopy structures as affecting factors on the process for throughfall drop generation, and estimated the influences of them, respectively. Fig. 1.2 shows the structure of this paper.

Chapter 2 describes the methodology of this study. The method measuring and calculating throughfall drops is shown. An instrument, a laser drop-sizing gauge (LD gauge), was newly developed to be optimized measuring throughfall drops.

Chapter 3 reassesses and rearranges the characteristics of drop size distribution and drop kinetic energy of throughfall. This chapter is based on the continuous and simultaneous observation in an unmanaged Japanese cypress plantation and open field.

Chapter 4 estimates the influence of canopy species and meteorological factors for throughfall drop generation. This chapter is based on the continuous and simultaneous observation under three different canopy species and open field.

Chapter 5 estimates the influence of canopy structures for throughfall drop generation. This chapter is based on the indoor experiment with artificial rainfall under a transplanted Japanese cypress tree.

I conclude this paper in Chapter 6.

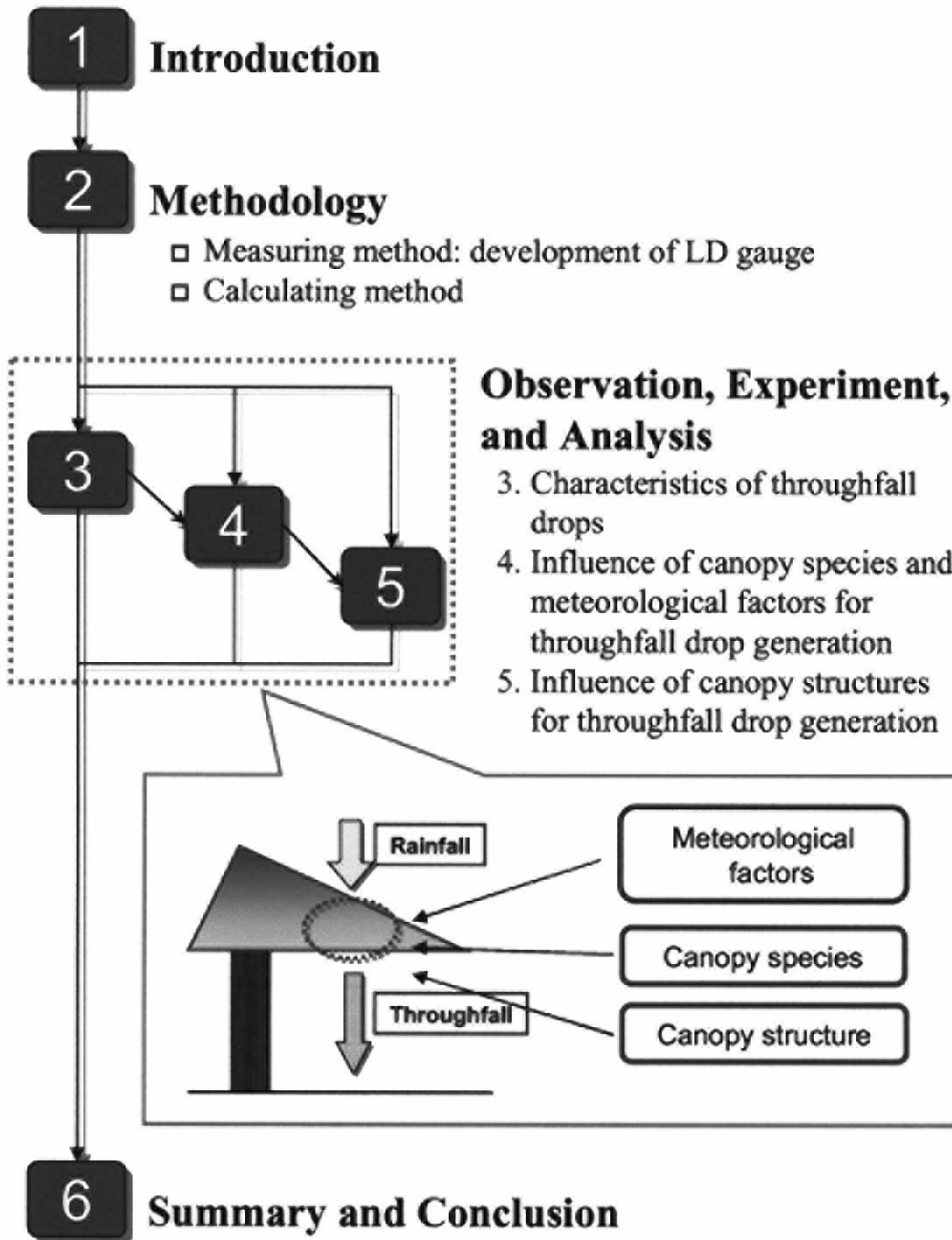


Figure 1.2 Structures of this paper.

Chapter 2

Methods for measuring and calculating throughfall drops

2.1 Measuring method of throughfall drops

2.1.1 Requirements for instruments to measure throughfall drops

There are some requirements for instruments to measure throughfall drops continuously. First, the instrument needs to have the automatic techniques by the optical method. Continuous drop measurements through one rainfall event are required to verify the drop size distribution (DSD) and to estimate drop kinetic energy with precision in a forest. The momentum method is commonly used to measure DSD and drop kinetic energy in open rainfall. Raindrop momentum is directly measured and raindrop diameter is calculated from momentum using the relationship between raindrop diameter and terminal velocity. Therefore, the method is invalid for throughfall drops because raindrops that drip from a low canopy may not always achieve terminal velocities. The optical method can monitor throughfall drops and has advantages over the other methods, in that it directly measures respective raindrop size and velocity.

Second, the instrument needs to realize the simultaneous and multiple measurements. More than two instruments are required estimating the characteristics of throughfall drops from the comparison with open rainfall drops, estimating the spatial variability of throughfall drops in same forested area, and estimating the influence of canopy species on throughfall drops. Additionally, the instrument is required small size, lightweight, inexpensive and easy to install because forested area in Japan usually placed in mountainous regions.

However, there have never been instruments meeting above requirements. A new laser drop-sizing gauge (named LD gauge) using the optical method was developed in this study. This chapter describes the methodology of measuring and calculating methods of throughfall drops.

2.1.2 Measuring principle of the LD gauge

A measuring principle of the LD gauge is based on the optical methods. The LD gauge consists of a paired laser optical transmitter and receiver, very small digital laser sensors (LX2-02; KEYENCE Co., Osaka, Japan), and an appropriate amplifier. Table 2.1 summarizes its specification. When a raindrop passes through the laser sheet emitted by the transmitter, the output voltage from the receiver is reduced in proportion to the intercepted area. Figure 2.1 shows an example of the temporal variations of output voltage from the laser sheet receiver. Each decrease of the output voltage was occurred by the two drops with different drop size and velocity. A large drop makes large interception area of the laser sheet. The voltage is converted into digital data with an A/D converter and stored on a PC connected to the LD gauge. Raindrop diameter is calculated from the relationship between the interception rate and the output voltage. Errors arising from the simultaneous presence of two or more drops in the sampling area were small. Martin and Joss (2000) showed that such errors were negligible, except during extremely intense rainfall exceeding 100 mm/h.

Each falling raindrop is assumed to be an oblate spheroid (Beard, 1976) whose flat ratio is determined using the equation in Pruppacher and Pitter (1971) as:

$$\frac{b}{a} = 1 \quad (D \leq 1 \text{ mm}) \quad (\text{Eq. 2.1})$$

$$\frac{b}{a} = 1.05 - 0.0655D \quad (D > 1 \text{ mm}) \quad (\text{Eq. 2.2})$$

where a is the major axis of an oblate spheroid (mm), b is the minor axis of an oblate spheroid (mm) and D is equivalent spheroid diameter (mm), calculated from the raindrop volume assuming sphericity.

From the drop size, the drop volume and precipitation are calculated. The volume of a drop ($Vol: \text{mm}^3$) was calculated as:

Table 2.1 Specifications of the laser sensor

Product name	KEYENCE LX2-02
Sensor head	
Size	
Transmitter	20 × 20 × 50 mm
Receiver	20 × 20 × 30 mm
Weight	
Transmitter	110 g
Receiver	90 g
Laser diode wavelength	780 nm
Power	3 mW
Power supply	24 V DC or 100 V AC
Light sheer size	10 × 1 mm (wide × thick)
Minimum detectable size	0.1 mm opaque object

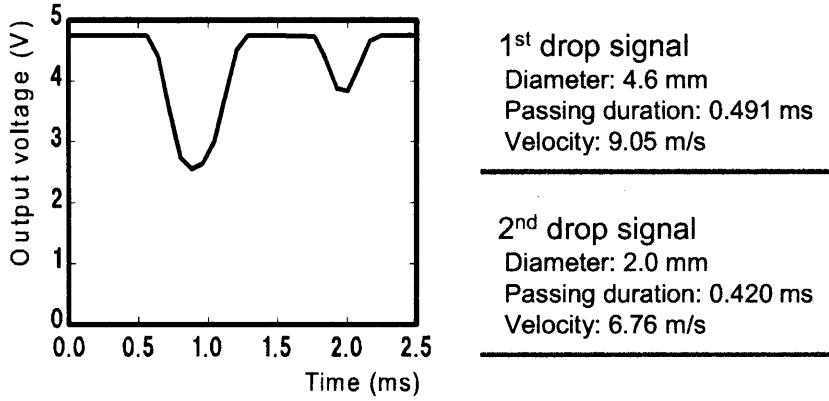


Figure 2.1 An example of the temporal variations of output voltage from the laser sheet receiver. Each decreases of the output voltage was caused by the two drops with different drop size and velocity.

$$Vol = \frac{4}{3}\pi \cdot \left(\frac{D}{2}\right)^3 = \frac{\pi}{6}D^3 \quad (\text{Eq. 2.3})$$

Therefore, precipitation in a definite period (R : mm) was calculated as:

$$R = \frac{1}{S} \cdot \sum_{i=1}^n Vol_i = \frac{\pi}{6} \cdot \frac{1}{S} \cdot \sum_{i=1}^n D_i^3 \quad (\text{Eq. 2.4})$$

where S is the sampling area of the LD gauge (mm^2), and n is the number of drops measured in a definite period.

2.1.3 Development of the LD gauge

Development

The LD gauge version 1 was produced in 2001 as in Yamada et al. (1996). Figure 2.2 shows the LD gauge version 1 and Table 2.2 summarizes its specification. The data acquisition interval was set at 0.04 ms. The LD gauge version 1 was smaller than those used in Yamada et al. (1996). The raindrop sampling area was fixed at $400 \text{ mm}^2 (= 4 \text{ cm}^2)$ in this study and varied from $600\text{--}3,000 \text{ mm}^2 (= 6\text{--}30 \text{ cm}^2)$ in Yamada et al. (1996). A cylinder was set to prevent raindrops from striking the sensors.

The LD gauge version 1 was used in the study described in 'Chapter 3'.

Drop size calibration

Drop size calibration of the LD gauge was achieved by dropping six sizes of glass sphere (mean diameters of 1.29, 1.91, 3.40, 3.95, 5.01 and 7.04 mm) through the laser sheet. The mean diameter of each bead was inferred from the increased volume of a fixed number of beads in a measuring

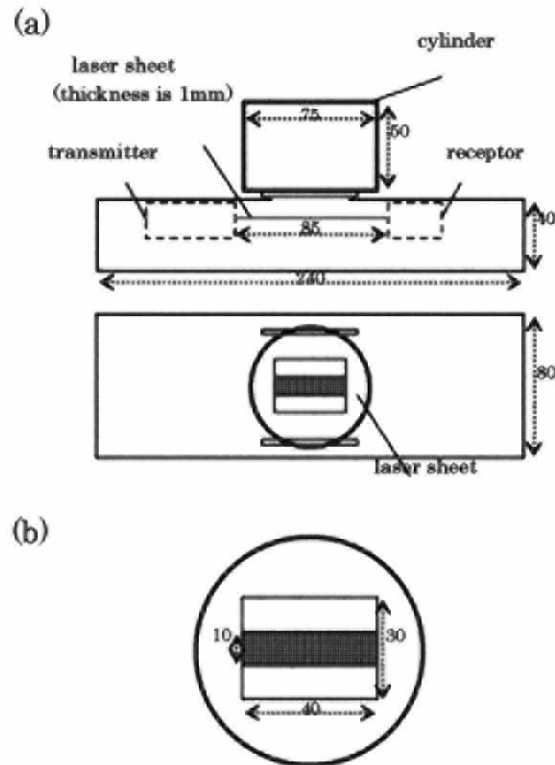


Figure 2.2 a Front and top views of the LD gauge version 1. b Top view of the sampling hole. Units are millimeters.

Table 2.2 Specifications of the LD gauge version 1

LD gauge version 1	
Size	80 × 40 × 240 mm
Sampling hole	30 × 40 mm
Sampling area	400 mm ² (10 × 40 mm)
A/D converter resolution	8 bit
Measuring range diameter	0.594 - 10 mm
Data acquisition interval	0.04 ms

cylinder. One hundred beads of each size were dropped through the sampling area, and the respective interception rates were recorded. Figure 2.3 summarizes the results and shows the linear relation between interception rate and glass sphere diameter as in following equation (a solid line in Fig. 2.3):

$$D_{bead} = 9.69I_C + 0.594 \quad R^2 = 0.985 \quad (\text{Eq. 2.5})$$

where D_{bead} is diameter of bead (mm) and I_C is the interception rate of the laser sheet.

The shape of falling raindrops was oblate spheroid but the shape of glass beads was approximately sphericity. On speculating D_{bead} from the interception rate, D_{bead} of a spherical particle is larger than that of an oblate spheroid particle. The difference enlarges in proportion to the interception rate. Accordingly, Eq. 2.5 should be corrected as following equation (a broken line in Fig. 2.3):

$$D = 8.747I_C + 0.561 \quad R^2 = 0.981 \quad (\text{Eq. 2.6})$$

where D is equivalent spheroid diameter (mm).

The reliability of the equation was confirmed falling actual water drops through a laser sheet (Fig. 2.3). The difference between D calculated from Eq. 2.6 and D calculated from the raindrop volume assuming sphericity did not exceed 5.0%. Experiments showed that the LD gauge version 1 could detect raindrops exceeding 0.561 mm in diameter.

Drop capture rate

The performance of the LD gauge was estimated on the drop capture rate. It was the rate of the precipitation between measured with a tipping-bucket raingauge and measured with the LD gauge in same rainfall event. The drop capture rate of the LD gauge was 2–12 % in three rainfall events observed in 2001, described in 'Chapter 3'.

The amount of precipitation varied on the sampling area. Smallness of sampling area may reduce the amount of precipitation measured. Kawabata (1961) showed that a circular raindrop collector exceeding 10 cm in diameter ($= 78.5 \text{ cm}^2$) assured an adequate sampling area for measuring rainfall amount. Note that setting up the cylinder above the sampling area may cause an error in observed precipitation (Ushiyama and Matsuyama, 1995; Sevruck and Nespor, 1998). The LD gauge does have some shortcomings for measuring total rainfall amount.

Figure 2.4 shows temporal fluctuations in one-hour rainfall intensity measured with the LD gauges and the tipping-bucket raingauge. The two sets of data for each rainfall event correspond well, with significance at the 5% level. This demonstrates that the LD gauges can determine qualitative DSD, and the capture rate during each rainfall event can be used to manipulate raindrop data quantitatively. Because the raindrop capture rate differed for each observation and site, the observed numbers of raindrops were divided by the raindrop capture rate before the analysis to eliminate variations in the capture rate.

2.1.4 Improvement of the LD gauge

The LD gauge version 2 was produced in 2002 improving the LD gauge version 1. Figure 2.5 shows

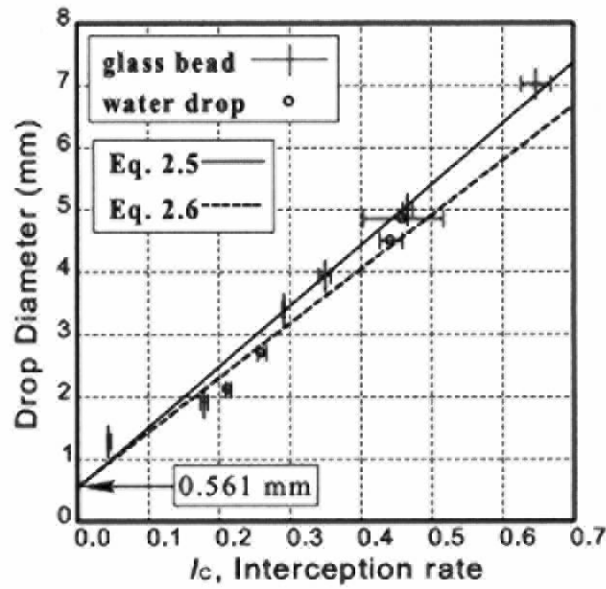


Figure 2.3 Calibration relationship between the interception rate and the glass sphere diameter (*vertical line*) for six different sizes and the water drop diameter (*circle*) for four different sizes.

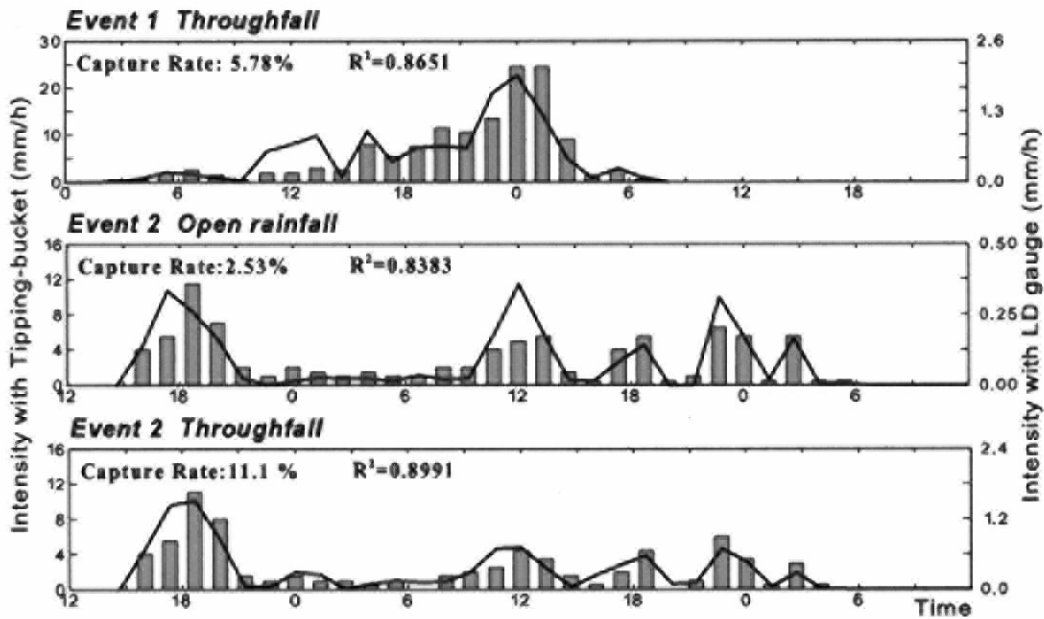


Figure 2.4 Comparison of the 1-h rainfall intensity between the tipping-bucket (*bar graph*) and the LD gauge (*line graph*) data. Each figure shows the raindrop capture rate and correlation coefficient.

the LD gauge version 2 and Table 2.3 summarizes its specification. It was equipped with a more moisture-proof case for the sensors according to the optical disdrometer developed by Martin and Joss (2000) and incorporated twice the drop sampling area ($= 800 \text{ mm}^2$) as compared to the earlier LD gauge. Furthermore, the cylinder above the sampling hole was removed because the cylinder intercepted raindrops entering the sampling hole with some inclination by wind. These improvements resulted in a high drop capture rate of over 95%, as measured against rain gauge capture. The reliability in drop sizing of the advanced LD gauges was confirmed by a calibration experiment using glass spheres and water drops likewise with the earlier LD gauge. Strong linearity between the drop size and interception rate was also confirmed for the LD gauges. The LD gauge in this study detected drops exceeding 0.532 mm in diameter.

The LD gauge version 2 was used in the studies described in 'Chapter 4' and 'Chapter 5'.

2.2 Calculating method of throughfall drops

Drop velocity

Raindrop velocity was calculated from the LD gauge's data as:

$$V_D = \frac{b + L - T_h}{t} \quad (\text{Eq. 2.7})$$

where V_D is the drop velocity (m s^{-1}), L is the width of laser sheer ($=1 \text{ mm}$), T_h is a necessary distance to detect a raindrop (mm), and t is intercepted time (ms) measured with the LD gauge. b is calculated from Eq. 2.1 and 2.2.

Drop kinetic energy

Drop kinetic energy is calculated by a raindrop weight and velocity. Raindrop kinetic energy (e : J) is calculated from a following equation as:

$$e = \frac{1}{2} m V^2 = \frac{1}{2} \rho \cdot \left(\frac{\pi}{6} D^3 \right) \cdot V_D^2 \quad (\text{Eq. 2.8})$$

where m is a raindrop weight (g), ρ is a raindrop density ($= 1 \times 10^{-6} \text{ g m}^{-3}$). Thus, the total amount of kinetic energy per unit area in a definite period (E : J m^{-2}) is calculated from a following equation as:

$$E = \frac{1}{S} \cdot \sum_{i=1}^n e_i \quad (\text{Eq. 2.9})$$

where S is sampling area of the LD gauge ($= 800 \text{ mm}^2 = 8 \times 10^{-4} \text{ m}^2$) and n is the number of drops measured during a definite period.

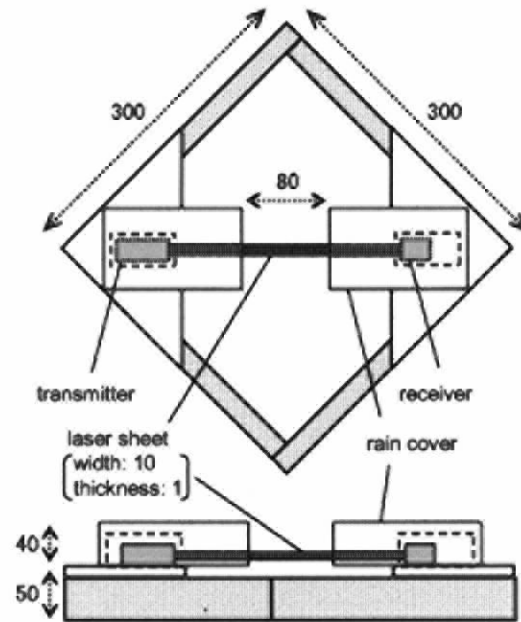


Figure 2.5 Top and front views of the LD gauge version 2. Units are millimeters.

Table 2.3 Specifications of the LD gauge version 2

LD gauge version 2	
Size	300 × 300 × 100 mm
Sampling area	800 mm ² (10 × 80 mm)
A/D converter resolution	8 bit
Measuring range diameter	0.540 - 10 mm
Data acquisition interval	0.04 ms

Chapter 3

Characteristics of throughfall drops: A field observation of throughfall in an unmanaged Japanese cypress plantation

3.1 Introduction

Soil erosion in unmanaged Japanese cypress (*Chamaecyparis obtusa*) plantations: Poorly managed mature Japanese cypress plantations in Japan suffered from surface erosion (Akenaga and Shibamoto, 1933; Kawana et al., 1963; Miura et al., 2002) and decreased infiltration rates (Yukawa and Onda; 1995) because of the lack of sufficient surface cover (Sakai and Inoue, 1988; Magarisawa et al., 1992). When considering soil surface erosion and crusting processes in such forests, it is necessary to determine the size distribution of throughfall drops, because the canopy produces large drops and promotes drops' erosive potential by increasing their kinetic energy (Chapman, 1948).

Estimation of drop size distribution and kinetic energy of throughfall: Previous studies showed that the throughfall drop size distribution (DSD) was independent of rainfall intensity (Mosley, 1982; Vis, 1986) and throughfall had a typical DSD (Tsukamoto, 1966; Brandt, 1989). However they used discontinuous data measured with manual methods, such as the stain method or the flour method; thus there were insufficient measurements of the changes in throughfall-DSD during temporal fluctuations in meteorological factors such as rainfall intensity. Furthermore, the calculation of drop kinetic energy was conceptual because of fragmentary drop data. Continuous drop measurements through one rainfall event are necessary to verify the throughfall-DSD and estimate drop kinetic energy in a forest with precision.

Objectives of this study: This study estimates and reconfirms throughfall-DSD and throughfall kinetic energy by comparisons between open rainfall and throughfall under a cypress canopy based on the continuous drop observations during rainfall events. We observed drops inside and outside a

mature Japanese cypress plantation simultaneously using several LD gauges.

3.2 Materials and methods

Site description

Observations were conducted at the University of Tokyo's University Forest, located in Chiba, in October 2001. Figure 3.1 shows the location map. We established two observation sites, a throughfall observation site (=TH, subsequently) and two open rainfall observation sites, R1 and R2. TH was under a mature Japanese cypress plantation, specifically at the Fukuroyamasawa Experimental Catchment. The catchment is about 60 km southeast of Tokyo at 35°12'N and 140°06'E at an elevation of 124-227 m asl. Mean annual rainfall is approximately 2,300 mm, and mean annual temperature is 14°C, 1941-1970. The cypress trees were planted in 1929. In a 1995 survey, tree density was 932 trees per hectare, the mean diameter at breast height (DBH) was 21.5 cm, and the mean tree height was 19.1 m. There was only a cypress canopy over TH because plants in the lower layer were cut down in September 1997. The first branch height of five trees adjoining TH was 14.9 m. Site TH has been used previously in studies of throughfall, stemflow, interception, and associated chemistry (e.g., Kuraji et al., 2001; Tanaka et al., 2005a; Tanaka et al., 2005b). Kuraji et al. (1998) determined that the annual throughfall rate of rainfall was about 75% during 1995-97.

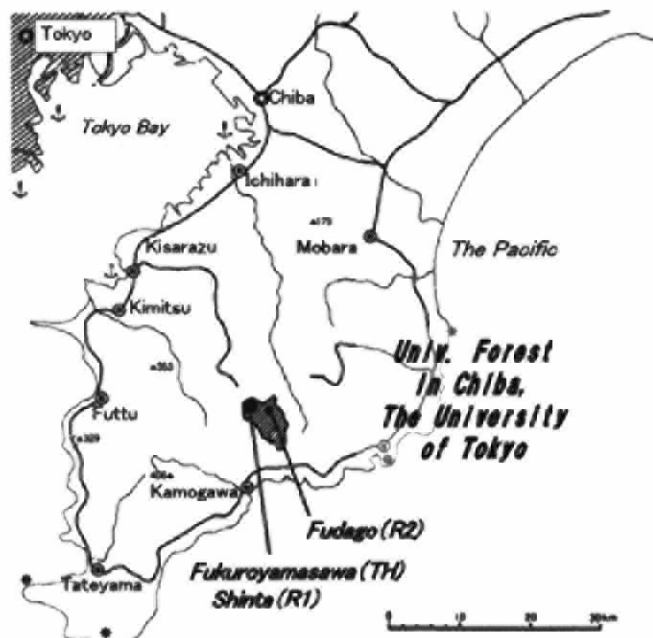


Figure 3.1 Study site locations.

Open rainfall was observed at two sites: R1 at the Shinta Weather Station, 200 m east of Fukuroyamasawa, and R2, at the Fudago Weather Station, 3.8 km northeast of Fukuroyamasawa.

Data collection

Table 3.1 lists the experimental sites and instrument set-up at each site. Precipitation was measured with 0.5-mm tipping-bucket raingauges (34-T; OTA KEIKI SEISAKUSHO, Co., Ltd., Tokyo, Japan); tip time was recorded with 0.5-s accuracy by a data logger (HOBO Event; Onset Computer Corp., Bourne, MA, USA). Raingauges were set-up at all of the sites. Drop size was measured with LD gauges version 1 (Fig. 2.2) on a platform 50 cm above the ground that was unaffected by drops reflected up from the surface. Throughfall drops were observed with two LD gauges to cancel the difference of the spatial distribution of throughfall drops. Open rainfall drops was observed with one LD gauge at R2 because of R2's accessibility and available electricity supply. Furthermore, the characteristic of respective observed rainfall events can be judged at R2 from previous open rainfall data that have been collected there since 1937. Rainfall data at R1 was used for comparison because of the proximity of TH and R1.

Throughfall spatial distribution is irregular compared with open rainfall (Nakakita, 1984; Lloyd and Marques, 1988; Sato et al., 2003), however, Tanaka et al. (2005b) resulted that the site in this study had little scattering in throughfall distribution by the experimentation using the grid of milk pack rain gauges. Thus we judged drops measured with the LD gauge could represent in observation area in spite of the small size of sampling area, 400 mm².

Methods of analysis

Drop size is measured with the LD gauge, but drop velocity was calculated in this study. We regarded that observed throughfall drops sufficiently reached terminal velocity, because there was no undergrowth and the canopy was sufficiently high (= 14.9 m). Wang and Pruppacher (1977) showed that raindrops exceeding 1.0 mm in diameter require a distance of at least 12 m to accelerate to terminal velocity.

Terminal velocity of drops was calculated with the equation in van Dijk et al. (2002a). van Dijk et al. (2002a) derived a simple terminal velocity equation that approximates previous empirical results under standard conditions of air pressure (1 bar) and air temperature (20°C) very well. The equation is

$$V_T = 0.0561D^3 - 0.912D^2 + 5.03D - 0.254 \quad (\text{Eq. 3.1})$$

where V_T is the terminal velocity of a drop (m s⁻¹) and D is the equivalent spherical diameter of a drop (mm). Factors other than raindrop diameter were ignored because air pressure and temperature differences in this study caused a maximum difference of only 1.2% in calculations using the physical equation in Beard (1976).

The calculating methods of drop size and kinetic energy were shown in 'Chapter 2'.

3.3 Results and Discussions

Rainfall events

Two rainfall events were monitored during the observation period in October 2001. The events were named Event 1 and Event 2, respectively. Table 3.1 and 3.2 compare the two events. Figure 3.2 shows temporal variation in rainfall intensity and drop size. Event 1 yielded 181.0 mm of open precipitation and an open-air maximum rainfall intensity of $10.0 \text{ mm } 10\text{-min}^{-1}$. There were no open-air drop data for the first event. Event 2 yielded 96.5 mm of precipitation and an open-air maximum intensity of $2.5 \text{ mm } 10\text{-min}^{-1}$. Event 2 had similar rainfall intensity transitions at R1 and R2, shown in Fig. 3.3. R1 and R2 were assumed to have similar DSD, despite the 3.8-km separation between the two open sites, because open drop distribution correlates with rainfall intensity (Marshall and Palmer, 1948). Throughfall precipitation during the two events was respectively 85 and 82% of the open rainfall at R1.

Comparison of throughfall and open rainfall

Figure 3.2b and Table 3.3 compare throughfall and open rainfall for Event 2. Drop sizes were different between open rainfall and throughfall. For open rainfall, large drops occurred when open rainfall intensity was high. The maximum open drop diameter was 3.31 mm and D_{50} , the median volume diameter, was 1.08 mm. In contrast, for throughfall, large drops were also observed at low rain intensities. Throughfall had larger drops than open rainfall. The maximum throughfall drop diameter was 6.35 mm and D_{50} was 4.42 mm. Throughfall drops were 4.1 times larger in D_{50} than open rainfall drops. Furthermore, drop number of throughfall was fewer than that of open rainfall. In

Table 3.1 Study sites and instrument set-up

	Raingauge	LD gauge		Distance from TH
		Event 1	Event 2	
		10 Oct 2001	17-18 Oct 2001	
TH: throughfall site	Y	Y	Y	—
R1: Open site 1	Y	no	no	200m
R2: Open site 2	Y	no	Y	3.8km

"Y" indicates the existence of each instrument measurement data and "no" indicates no data.

Table 3.2 Rainfall events

Event	Date	Precipitation (mm)				Maximum intensity ^a (mm 10-min^{-1})	
		R2	R1	TH	(TH/R1)	R2	TH
		1	10 Oct 2001	181.0	160.0	136.0	(85.0 %)
2	17-18 Oct 2001	96.5	92.5	76.0	(82.2 %)	2.5	2.5

All data observed with 0.5-mm tipping bucket raingauges

^a The maximum 10-min rainfall intensity

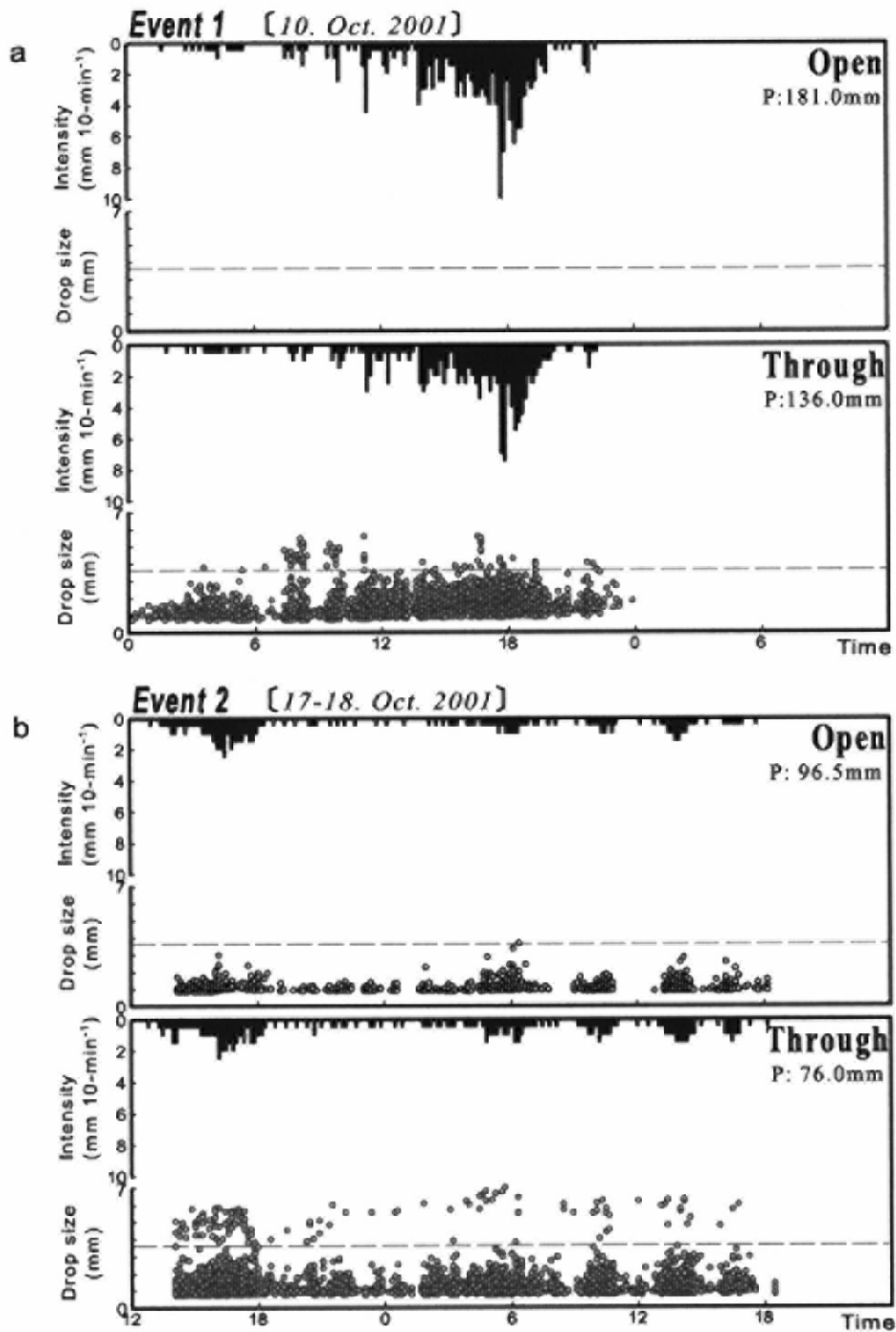


Figure 3.1 Temporal transition in rainfall intensity and drop size. The *broken lines* indicate 3.31 mm, the maximum diameter of open rainfall drops in this observation. *P* indicates the total precipitation for rainfall events, Event 1 (a) and Event 2 (b).

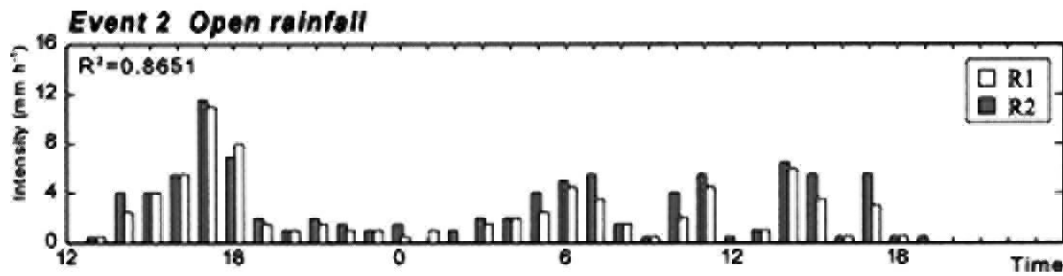


Figure 3.3 Comparison of the 1-h rainfall intensity between R1 and R2 measured with the tipping-bucket raingauges.

the LD gauge sampling area (400 mm^2), 59,033 open rainfall drops and 10,732 throughfall drops were counted. These results suggest that raindrops coalesced in the canopy, forming larger throughfall drops.

Figure 3.4a shows the DSDs of open rainfall and throughfall based on the drop volume. A clear difference exists between open rainfall and throughfall. In open rainfall, precipitation is mostly consisted of small drops around 1 mm in diameter. Drops less than 2 mm in diameter comprised 87.2% of the precipitation by volume. In contrast, throughfall included drops of various sizes. Throughfall drops exceeding 3.31 mm in diameter, the maximum drop diameter in open rainfall, comprised 3.0% of the number of drops, but 63.8% of the total volume.

Drop impact energy can be approximated from the kinetic energy of falling drops. Figure 3.4b compares the kinetic energy of open rainfall and throughfall during Event 2. Although throughfall precipitation was 85% smaller than open rainfall (Table 3.2), the kinetic energy of throughfall was over twice that of open rainfall. Unit kinetic energy, the mean kinetic energy at 1 mm in precipitation, during one rainfall event was $11.9 \text{ J m}^{-2} \text{ mm}^{-1}$ in open rainfall and $32.5 \text{ J m}^{-2} \text{ mm}^{-1}$ in throughfall. Large drops had a large percentage of the throughfall in Event 2. As drops increase in size, they fall faster, gaining larger kinetic energy. Thus, the throughfall kinetic energy increases. A forest canopy increases the risk of surface erosion for a bare ground surface.

Comparison of two throughfall events

Two throughfall events were compared using data for Events 1 and 2. Table 3.4 summarizes the throughfall data for the two events. Event 2 yielded 40% less precipitation, and it also had lower rainfall intensity than Event 1. During open rainfall, greater rainfall intensity produced larger drops; thus Event 1 would have larger drops than Event 2. However, throughfall showed opposite results from the expectation. Large drops occurred fewer in Event 1 than Event 2 (Fig. 3.3). Throughfall drops exceeding 6 mm in diameter were generated only during a lower rainfall intensity event, Event 2. For Event 1, the maximum drop diameter was 5.07 mm and D_{50} was 2.05 mm.

A clear difference exists in DSDs between two throughfall events. Figure 3.5a shows the DSDs of two throughfall events based on the drop volume. During Event 1, there were more drops 1.0–3.0 mm in diameter than any other diameter class; their volume accounted for 73.7% of the precipitation. Conversely, during Event 2, there were many drops over 4.0 mm in diameter and their volume

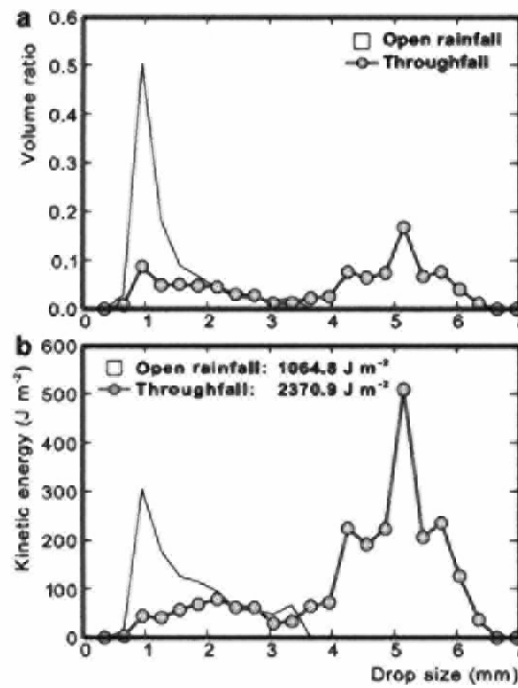


Figure 3.4 Drop size distributions of open rainfall and throughfall in Event 2, based on drop volume (a) and based on kinetic energy (b).

Table 3.3 Comparison of open rainfall and throughfall in Event 2

	Precipitation (mm)	Drop size (mm)		Drop number (in 400 mm^2)	Kinetic energy	
		Maximum	D_{50}		Total (J m^{-2})	Unit ($\text{J m}^{-2} \text{ mm}^{-1}$)
Open	96.5	3.31	1.08	59 033	1064.8	11.0
Throughfall	76.0	6.35	4.42	10 732	2370.9	31.2

Each site had the same maximum rainfall intensity of $2.5 \text{ mm } 10\text{min}^{-1}$

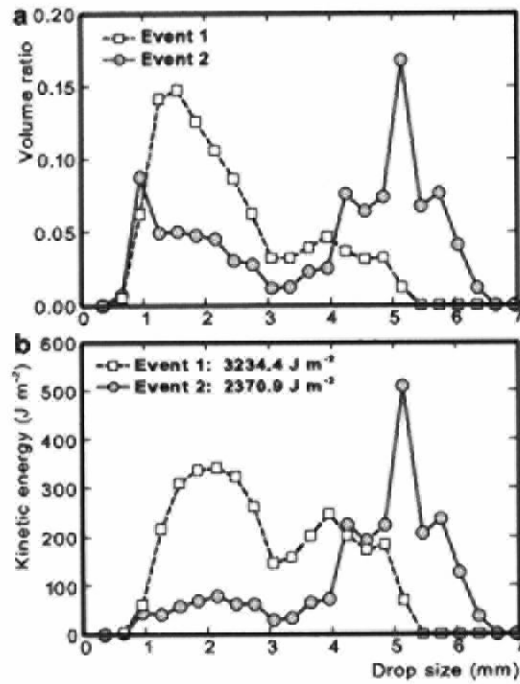


Figure 3.5 Drop size distributions of throughfall in Event 1 and Event 2, based on drop volume (a) and based on kinetic energy (b).

Table 3.4 Comparison of two throughfall events in Event 1 and 2

Event	Precipitation (mm)	Maximum intensity (mm 10-min ⁻¹)	Drop size (mm)		Kinetic energy	
			Maximum	D_{50}	Total ($J m^{-2}$)	Unit ($J m^{-2} mm^{-1}$)
1	136.0	7.5	5.07	2.05	3234.4	23.8
2	76.0	2.5	6.35	4.42	2370.9	31.2

accounted for 58.6% of the precipitation. Thus, throughfall did not have the same DSD during different events, countering to the results of previous studies (e.g. Tsukamoto, 1966; Mosley, 1982; Brandt, 1989). We suspect that a shortage of coalescing processes in drops dripping from the canopy during high rainfall intensity is a likely cause. High rainfall intensity increases the impact energy of drops striking the canopy; the greater impact energy may cause the canopy to vibrate, thus inhibiting large drop formation.

The throughfall kinetic energy was also different between two events. Figure 3.5b shows the DSDs of two throughfall events based on the drop kinetic energy. The total kinetic energy was 3234.4 J m⁻² in Event 1 and 2370.9 J m⁻² in Event 2. Event 1 had larger total kinetic energy than Event 2 because of largeness of the precipitation. However, the unit kinetic energy of Event 1 was, in contrast, lower than that of Event 2, 23.8 J m⁻² mm⁻¹ in Event 1 and 31.2 J m⁻² mm⁻¹ in Event 1. The throughfall precipitation in Event 1 was consisted of smaller drops, 1.0–3.0 mm in diameter, than that in Event 2. Such drops have little kinetic energy and do not cause a marked increase in drop impact energy. Conversely, drops over 4.0 mm in diameter in Event 2 had large kinetic energy, which increased the total kinetic energy.

Figure 3.6 shows the increase in drop kinetic energy with precipitation. If throughfall DSD was independent of rainfall intensity, the cumulative kinetic energy should be proportional to the precipitation amount (Miura et al., 2002) and should increase uniformly along the fine solid line in Fig. 3.6. However, the total mean slope (the fine solid lines in Fig. 3.6) varied between Events 1 and 2. Furthermore, the drop kinetic energy in Event 1 had varying slopes and changes, whereas the drop kinetic energy in Event 2 showed a nearly constant increase according to the amount of precipitation. Throughfall did not have the uniform DSD in the two events or among different periods of time in one rainfall event

In Figure 3.6, there are three inflection points for Event 1: two points where the slope changes gently (circle and square) and one point where the slope changes abruptly (triangle). The gentle slope changes when the rainfall intensity jumping increased, from 0.5 to 3.0 mm 10-min⁻¹ at the first point and from 2.5 to 7.0 mm 10-min⁻¹ at the second point. Consequently it is possible that a sudden transition of throughfall intensity from low to high changes the distribution of throughfall drops.

3.4 Conclusions

Throughfall and open rainfall drops were observed continuously within and outside a Japanese cypress plantation. Comparison of throughfall and open rainfall for one rainfall event suggested the following: 1) Throughfall drops were fewer in number, but larger in size, than open rainfall drops for one rainfall event; 2) Large drops were scarce in open rainfall but accounted for about half of the throughfall precipitation. Raindrops coalesce in the canopy; 3). The drop impact energy increased as large drops were produced.

Comparison of the two throughfall events suggested that the throughfall drops did not always have the uniform distribution in different events or in different time periods in one rainfall event, in contrast to the previous studies which resulted that throughfall drops had the uniform size distribution independent of rainfall intensity.

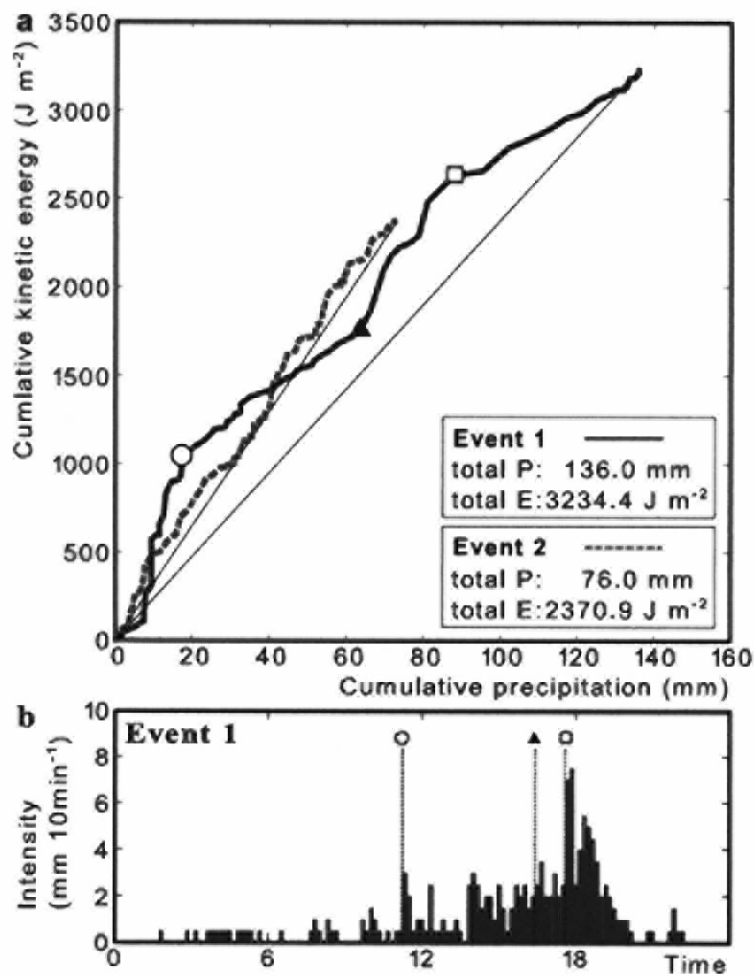


Figure 3.6 a Relationship of the cumulative precipitation and cumulative kinetic energy during Event 1 and Event 2. At the *circle* and *square*, the slope changes gently, and at the *triangle* the slope changes abruptly. b Temporal variation in throughfall rainfall intensity in Event 1. Each *symbol* links to the *symbol* in the top figure.